EXPERIMENTAL CELL RESEARCH 318 (2012) 1685–1698

Available online at www.sciencedirect.com

SciVerse ScienceDirect

journal homepage: www.elsevier.com/locate/yexcr

Research Article

The hypoxia-inducible factor-responsive proteins semaphorin 4D and vascular endothelial growth factor promote tumor growth and angiogenesis in oral squamous cell carcinoma

Hua Zhou[a], *Ying-Hua Yang*[a], *Nada O. Binmadi*[a,b], *Patrizia Proia*[a,c], *John R. Basile*[a,d,*]

[a]*Department of Oncology and Diagnostic Sciences, University of Maryland Dental School, 650W. Baltimore Street, 7-North, Baltimore, MD 21201, USA*
[b]*Department of Oral Basic & Clinical Sciences, King Abdulaziz University, Jeddah 21589, Saudi Arabia*
[c]*Department of Sports Science (DISMOT), University of Palermo, Via Eleonora Duse 2 90146, Palermo, Italy*
[d]*Greenebaum Cancer Center, 22S. Greene Street, Baltimore, MD 21201, USA*

ARTICLE INFORMATION

Article Chronology:
Received 27 January 2012
Received in revised form
19 March 2012
Accepted 10 April 2012
Available online 29 May 2012

Keywords:
Semaphorin 4D
Plexin-B1
VEGF
Oral squamous cell carcinoma
Angiogenesis
HIF

ABSTRACT

Growth and metastasis of solid tumors requires induction of angiogenesis to ensure the delivery of oxygen, nutrients and growth factors to rapidly dividing transformed cells. Through either mutations, hypoxia generated by cytoreductive therapies, or when a malignancy outgrows its blood supply, tumor cells undergo a change from an avascular to a neovascular phenotype, a transition mediated by the hypoxia-inducible factor (HIF) family of transcriptional regulators. Vascular endothelial growth factor (VEGF) is one example of a gene whose transcription is stimulated by HIF. VEGF plays a crucial role in promoting tumor growth and survival by stimulating new blood vessel growth in response to such stresses as chemotherapy or radiotherapy-induced hypoxia, and it therefore has become a tempting target for neutralizing antibodies in the treatment of advanced neoplasms. Emerging evidence has shown that the semaphorins, proteins originally associated with control of axonal growth and immunity, are regulated by changes in oxygen tension as well and may play a role in tumor-induced angiogenesis. Through the use of RNA interference, *in vitro* and *in vivo* angiogenesis assays and tumor xenograft experiments, we demonstrate that expression of semaphorin 4D (SEMA4D), which is under the control of the HIF-family of transcription factors, cooperates with VEGF to promote tumor growth and vascularity in oral squamous cell carcinoma (OSCC). We use blocking antibodies to show that targeting SEMA4D function along with VEGF could represent a novel anti-angiogenic therapeutic strategy for the treatment of OSCC and other solid tumors.

Abbreviations: SEMA4D, semaphorin 4D; sSEMA4D, soluble SEMA4D; AP, alkaline phosphatase; VEGF, vascular endothelial growth factor; HIF, hypoxia inducible factor; OSCC, oral squamous cell carcinoma; HUVEC, human umbilical vein endothelial cell; shRNA, short hairpin RNA; FBS, fetal bovine serum; BSA, bovine serum albumin; CM, conditioned media; ERK, extracellular signal regulated kinase; BME, basement membrane extract

*Corresponding author at: Department of Oncology and Diagnostic Sciences, University of Maryland Dental School, 650 West Baltimore Street, 7-North, Baltimore, MD 21201, USA. Fax: +1 410 706 0519.
E-mail address: jbasile@umaryland.edu (J.R. Basile).

0014-4827/$ - see front matter © 2012 Elsevier Inc. All rights reserved.
http://dx.doi.org/10.1016/j.yexcr.2012.04.019

Introduction

Oral squamous cell carcinoma (OSCC) is the sixth most common cancer among men in the developed world and among the most fatal cancers at any anatomic site [1]. Because even advanced lesions are usually not painful to the patient, OSCC in areas that cannot be easily visualized such as the lateral and ventral tongue and the posterior oropharynx in particular can evade early detection, eventually requiring aggressive surgical intervention and chemo- or radiotherapy to establish local control. Like many other solid tumors, OSCC lesions represent a heterogeneous population of genetically labile malignant cells that can evolve mutations under the strong selective pressures of such cytotoxic therapies, leading to the emergence of resistant cell populations and eventual treatment failure. A promising alternative treatment strategy is anti-angiogenic therapy, which instead targets the endothelial cells that line the vessels that feed the tumor, thus bypassing complications such as resistance to chemotherapy that can arise in a background of genetic instability when targeting cancer cells themselves.

Growth and metastasis of solid tumors requires induction of angiogenesis, the creation and remodeling of new blood vessels from a pre-existing vascular network, to ensure the delivery of oxygen, nutrients and growth factors to rapidly dividing transformed cells. Without the ability to induce angiogenesis, most neoplasms would fail to grow larger than 2 mm in diameter or metastasize [2]. One way tumor cells acquire the ability to induce angiogenesis, and hence to grow and metastasize, is through activity of the hypoxia-inducible factor (HIF) family of transcription regulators, the most important effectors of the adaptive response to hypoxia in multicellular organisms. Initially identified by Semenza and colleagues in the early 1990s, the HIF transcriptional complex is composed of two polypeptides: the α and β subunits [3]. While the β subunit is expressed constitutively, HIF activity is regulated at the posttranscriptional level by the α subunits, which are stabilized or degraded in conditions of low or high oxygen tension, respectively [4]. As an active dimer, HIF binds to hypoxia response elements within the promoters of target genes resulting in the activation of a pro-survival program that opposes apoptosis, inhibits generation of reactive oxygen species, and activates the transcription of pro-angiogenic proteins such as vascular endothelial growth factor (VEGF). In OSCC, high levels of the HIF-1α subunit are correlated with poor prognosis [5], reduced disease-specific survival [6] and tumor progression, including enhanced size of primary lesion and lymph node metastasis [7]. HIF-1α is also over-expressed in the majority of patients with squamous cell carcinoma of the oropharynx and here too is correlated with a lower rate of remission, greater incidence of lymph node metastases, and poorer disease-free and overall survival [8].

The semaphorins and their receptors, the plexins, are a family of proteins characterized by cysteine-rich semaphorin domains originally identified as regulators of axon guidance and lymphocyte activation [9–11]. Our group and others have shown that semaphorin 4D (SEMA4D) is produced and secreted by the transformed cells of many different aggressive carcinomas, including OSCC, and that it acts through its receptor, Plexin-B1, on endothelial cells to promote angiogenesis and enhance tumor growth and survival [12–14]. Why SEMA4D is over-expressed in so many different tumor types remains unknown, but studies demonstrate that like other pro-angiogenic factors, plexins and semaphorins are regulated by changes in oxygen tension [15–18]. Indeed, we have previously shown that Sema4D is induced by hypoxia in a HIF-1-dependent manner and may be another route by which carcinomas promote angiogenesis [18].

The focus of the current study is to investigate the role of HIF-mediated SEMA4D induction in the generation of the pro-angiogenic phenotype in OSCC and determine its biological significance for tumor growth and vascularity when compared to, and in combination with, the better-studied angiogenic factor VEGF. Here we use lentiviral-mediated RNA interference and over-expression techniques, *in vitro* and *in vivo* angiogenesis assays and tumor xenografts to show that both VEGF and SEMA4D transcription is under the control of HIF and cooperate to promote angiogenesis for the purposes of enhancing vascular density and tumor cell proliferation in OSCC. We employ blocking antibodies to demonstrate that targeting SEMA4D along with VEGF might represent a new complementary or parallel mode of treatment for anti-angiogenic therapy of OSCC or other solid neoplasms.

Materials and methods

Cell culture

Human umbilical vein endothelial cells (HUVEC, ATCC, Manassas, VA), 293T cells (ATCC), and the head and neck (HN) squamous cell carcinoma cell lines HN12, HN13, and HN30 [19] were cultured in DMEM (Sigma, St. Louis, MO) supplemented with 10% fetal bovine serum and 100 units/ml penicillin/streptomycin/amphotericin B (Sigma).

Immunoblots

Cells infected with lentiviruses expressing the indicated constructs, treated with increasing concentrations of anti-SEMA4D blocking antibody 1.5 h prior to incubation with soluble SEMA4D (sSEMA4D) for 3 min (to determine ERK phosphorylation), or treated with up to 400 ng/ml sSEMA4D under conditions of low serum (to measure caspase 3 activation), were lysed in buffer (50 mM Tris–HCl, 150 mM NaCl, 1% NP 40) supplemented with protease inhibitors (0.5 mM phenylmethylsulfonyl fluoride, 1 μl/ml aprotinin and leupeptin, Sigma) and phosphatase inhibitors (2 mM NaF and 0.5 mM sodium orthovanadate, Sigma) for 15 min at 4 °C. After centrifugation, protein concentrations were measured using the Bio-Rad protein assay (Bio-Rad, Hercules, CA). 100 μg of protein from each sample was subjected to SDS-polyacrylamide gel electrophoresis and transferred onto a PVDF membrane (Immobilon P, Millipore Corp., Billerica, MA). The membranes were then incubated with the appropriate antibodies. The antibodies used were as follows: SEMA4D (BD Transduction Labs, BD Biosciences, Palo Alto, CA); VEGF (Santa Cruz Biotechnology, Santa Cruz, CA); HIF-1β (BD Transduction Labs); Tubulin (Santa Cruz Biotechnology); Total ERK (Cell Signaling Technology, Danvers, MA); Phospho-ERK (Cell Signaling Technology); Plexin-B1 (Santa Cruz A8); cleaved caspase 3 (Cell Signaling, Danvers, MA); GAPDH (Sigma). Proteins were detected using the ECL chemiluminescence system (Pierce, Rockford, IL).

Short hairpin (sh) RNA and lentiviral infections

The shRNA sequences for HIF-1β and Plexin-B1 were obtained from Cold Spring Harbor Laboratory's RNAi library (RNAi Central, http://cancan.cshl.edu, last accessed 3/13/12) [20,21]. The sequences used as PCR templates have been previously reported [18]. Oligos were synthesized (Invitrogen, Carlsbad, CA) and cloned into pWPI GW, a Gateway compatible CSCG based lentiviral destination vector, as previously described [14,18]. Viral stocks were prepared in 293T cells and infections per formed as previously reported [14,18]. For over-expression, VEGF (the generous gift of Dr. Qiangming Sun) and SEMA4D were cloned into pSHAG MAGIC2, an entry vector for the Gateway cloning system, and then an LR reaction was performed to transfer the inserts into pWPI GW (Invitrogen), as previously described [22].

Production of soluble SEMA4D

sSEMA4D was produced and purified as described previously [13]. Briefly, the extracellular portion of SEMA4D was subjected to PCR and the resulting product cloned into the plasmid pSecTag2B (Invitrogen). This construct was transfected into 293T cells growing in serum free media. Media containing sSEMA4D was collected 65 h. post-transfection and purified with TALON metal affinity resin (Clontech Laboratories, Palo Alto, CA) according to manufacturer's instructions. Concentration and purity of the TALON eluates was determined by SDS PAGE analysis followed by silver staining (Amersham Life Science, Piscataway, NJ) and the Bio-Rad protein assay (Bio-Rad, Hercules, CA). In all cases, media collected from cells transfected with the empty pSecTag2B vector were used as control.

VEGF and SEMA4D ELISA

VEGF and SEMA4D ELISAs were performed using the DuoSet ELISA development kit (R&D Systems) following the manufacturer's protocol. Briefly, the capture antibody was coated overnight in PBS at room temperature, followed by washing, blocking with 1% BSA for 1 h and incubation with 100 μl of sample, diluted 1:5, for 2 h at room temperature. Wells were then washed and 100 μl of detection antibody added for 2 h, followed by incubation with 100 μl of streptavidin-HRP for 20 min. Substrate and stop solutions were then added for the final steps. The concentrations of SEMA4D and VEGF were determined based on a standard curve and expressed as pg/ml. Each experiment was performed three times and average and standard deviation calculated.

In vitro migration assay

Serum free media containing 0.1% BSA (negative control), 10% FBS (positive control), sSEMA4D with and without blocking antibody, or media conditioned by HN12, HN13, and HN30 cells, control infected or infected with the indicated lentivirus constructs, was placed in the bottom well of a Boyden chamber while serum free media containing migrating HUVEC were added to the top chamber. The two chambers were separated by a polyvinylpyrrolidone membrane (8 μm pore size, Osmonics; GE Water Technologies, Trevose, PA) and the migration assay performed as described [13]. Cell migration was expressed as membrane staining intensity relative to negative control wells. Each experiment was performed three times and average and standard deviation calculated.

In vivo tubulogenesis assay

HUVEC were grown in 35 mm plates coated with 150 μl of Cultrex basement membrane extract (BME, Trevigen, Gaithersburg, MD) and incubated overnight in serum free media containing 0.1% BSA (negative control), 10% FBS (positive control), sSEMA4D with and without blocking antibody, or in media conditioned by control HN12, HN13, and HN30 cells or cells infected with the indicated lentivirus constructs. Cells were then fixed in 0.5% glutaraldehyde and photographed. Quantification of results was determined using ImageJ (NIH, Bethesda, MD, version 1.46c), measuring and summing the length of all tubular structures observed in 10 random fields for three independent experiments.

Directed *in vivo* angiogenesis assay (DIVAA)

A DIVAA assay (Trevigen) was performed as previously described [23] with modifications. Briefly, angioreactors were filled with 18 μl of Cultrex BME (Trevigen) containing PBS (negative control), 50 ng VEGF mixed with 150 ng basic fibroblast growth factor (positive control), or serum free media conditioned by control HN12 cells or cells infected with the indicated lentivirus constructs, and implanted subcutaneously into both flanks of immunocompromised (nude) mice. After 9 days, the mice were sacrificed and the angioreactors removed, photographed and processed with FITC-labeled Griffonia lectin (FITC-lectin), an endothelial cell selective reagent [24,25], to quantify invasion of endothelial cells into the lumen of the angioreactors. Fluorescence was determined in a plate reader as mean relative fluorescence units for four reactors.

Tumor xenografts

Two million HN12 cells, uninfected, control infected or infected with the indicated lentiviral constructs, were resuspended in 250 μl of serum free DMEM with an equal volume of Cultrex BME (Trevigen) and injected subcutaneously into both flanks of a host nude mouse, with 10 mice used per experimental condition. In the blocking antibody experiments, each mouse received i.p. injections of either 100 μg of anti-VEGF antibody (R&D Systems, Minneapolis, MN) or 100 μg of anti-SEMA4D antibody (VX15, which reacts with both human and mouse SEMA4D, Vaccinex, Rochester, NY), or both, where indicated, post-engraftment. As negative controls, tumor-bearing mice were also treated with IgG4 and IgG2a. Control antibodies were added to the treatment groups to match the total amount of protein delivered in the combination groups. Tumor volume was measured throughout the duration of all experiments. The animals were then sacrificed and tumors removed, photographed, weighed and processed for immunohistochemistry or immunofluorescence (see below). All animal studies were approved by the University of Maryland Office of Animal Welfare, Institutional Animal Care and Use Committee, in accordance with the NIH Guide for the Care and Use of Laboratory Animals.

Immunohistochemistry

Formalin fixed, paraffin embedded tumor tissues harvested from xenografted mice were processed for immunohistochemistry as previously described [26]. Briefly, tissues were deparaffinized, hydrated, rinsed with PBS, blocked in Power Block (BioGenex, Fremont CA), and incubated overnight at 4 °C with the indicated primary antibodies. The antibodies used were: Anti-HIF-1β (BD Transduction Laboratories; 1:100 dilution in 2% BSA/0.1% Tween 20 in PBS); Anti-SEMA4D (BD Transduction Laboratories; 1:50 dilution); Anti-VEGF (Santa Cruz Biotechnology, 1:50 dilution); Anti-Ki-67 (Santa Cruz Biotech, 1:50 dilution). The slides were then washed in PBS, incubated with biotinylated secondary antibody (Biotinylated Link Universal, DAKO North America) for 45 min, and treated with strepavidin-HRP (DAKO North America) for 30 min at room temperature. The slides were developed in 3,3-diaminobenzidine (FASTDAB tablets; Sigma), counterstained with dilute Mayer's hematoxylin, dehydrated, and mounted. Images were taken with an Aperio ScanScope CS scanner (Aperio, Vista, *CA*). Ki-67 results were determined by the percentage of positive nuclei in 10 high-power microscopic fields (at 100×), expressed as an average and standard deviation, taken from areas of the tumor that were not necrotic.

Immunofluorescence

Tumor tissues were processed for immunofluorescence as described [26]. Briefly, OCT-embedded 8 μm thick frozen tissue sections were cut onto silanated glass slides, air-dried, and stored at −80 °C. Cryosections were thawed, hydrated, fixed, blocked in 10% FBS, and incubated overnight at 4 °C with primary antibody diluted in a 2% BSA/0.1% Tween 20 solution in PBS. The antibodies used were as follows: Anti-CD31 (anti-PECAM, BD Pharmingen; 1:100 dilution); Anti-cleaved caspase 3 (Cell Signaling, 1:200 dilution). After washing with PBS, the slides were incubated with FITC-conjugated anti-rat (Sigma) or Texas red-conjugated anti-rabbit (Calbiochem, EMD Biosciences, San Diego, CA) secondary antibodies for 1 h at room temperature and mounted with Vectashield mounting medium with 4′,6-diamidino-2-phenylindole (DAPI, Vector Laboratories, Burlingame, *CA*). Slides were examined with a Nikon Eclipse E800 microscope system. Blood vessel content was determined by the average number of vessels in 10 high-power fields in CD31-stained xenografts, while vessel apoptosis was scored by expressing as a percentage the number of CD31 positive vessels co-staining with active cleaved caspase 3 in 10 high-power fields.

Alkaline phosphatase receptor binding assay

Alkaline phosphatase-fused sSEMA4D (AP-sSEMA4D) was used as a ligand for a receptor binding assay. A DNA fragment corresponding to amino acid residues 1-634 of human SEMA4D was cloned into the N-terminal portion of the human alkaline phosphatase (AP) gene in the vector AP Tag-5 (GenHunter Inc., Nashville, TN). This construct was transfected into 293FT cells using FuGENE HD (Roche Diagnostics, Indianapolis, IN) and the resulting protein purified from conditioned media with TALON metal affinity resin (Clontech Laboratories), as described previously [13]. In order to examine the effect of anti-SEMA4D antibody on binding of AP-sSEMA4D to Plexin-B1, the antibody was added to HUVEC, control infected or infected with lentivirus expressing Plexin-B1 shRNA (see above), 1.5 h. prior to addition of 1 μg/ml AP-sSEMA4D. After 1 h treatment, the cells were washed and solubilized by lysis buffer containing triton X-100, with bound AP-sSEMA4D quantified by AP activity in a colorimetric assay using the Sensolyte pNPP alkaline phosphatase assay kit (AnaSpec, Fremont, CA).

Statistical analysis

Student's paired *t*-tests were performed on means, and *p*-values calculated: * $p<0.05$; ** $p<0.01$.

Fig. 1 – HIF-mediated expression of SEMA4D and VEGF by OSCC cooperate to promote a pro-angiogenic response *in vitro*. (A) HN cells were infected with control lentiviruses or lentiviruses coding for HIF-1β shRNA, to eliminate expression of the β subunit of the HIF transcriptional complex, followed by lentiviral-mediated re-expression of VEGF, SEMA4D, or both, to selectively restore expression of these proteins and evaluate their individual and combined effects on angiogenesis, tumor growth and tumor vascularity. (B) HN12 cells exhibit loss of HIF-1β protein in an immunoblot following infection with lentivirus coding for HIF-1β shRNA. (C) HN12 cells were infected with control lentivirus, virus coding for HIF-1β shRNA, or virus coding for full-length SEMA4D (SEMA4D: +), as indicated, and blotted for SEMA4D. (D) HN12 cells were infected with control lentivirus, virus coding for HIF-1β shRNA, or virus coding for full-length VEGF (VEGF: +), as indicated, and blotted for VEGF. Tubulin was used as a loading control for all blots. (E) ELISA for secreted SEMA4D and VEGF performed on media conditioned by control infected HN12, 13 and 30 cells, cells infected with lentivirus coding for HIF-1β shRNA, or those cells co-infected with virus coding for SEMA4D and/or VEGF, as indicated, with results expressed as pg/ml (*Y*-axis). (F) HUVEC cells were examined in a Boyden chamber for migration toward 0.1% BSA (negative control), 10% FBS (positive control), or media conditioned by HN12 cell populations described in (A). Representative photos of stained migration assay membranes are shown. (G) Results of the Boyden chamber assay for HUVECS towards BSA, FBS, or media conditioned by HN12 (red bars), HN13 (blue bars) and HN30 (green bars), treated as indicated, expressed as pixel intensity of scanned stained migration membranes relative to negative controls. Error bars represent the standard deviation from three independent experiments (* $p<0.05$; ** $p<0.01$). (H) HUVEC cells were plated on reconstituted basement membrane material in serum free media with 0.1% BSA (negative control), 10% FBS (positive control), or media conditioned by HN cell populations described in (A) and examined for formation of capillary tubes. (I) Quantification of HUVEC tube formation in the presence of BSA, FBS, or media conditioned by HN12 (red bars), HN13 (blue bars) and HN30 (green bars), treated as indicated, measuring and summing the length of all tubular structures observed in 10 random fields. Error bars represent the standard deviation from three independent experiments (* $p<0.05$; ** $p<0.01$).

Results

HIF-mediated expression of SEMA4D by OSCC combines with VEGF to elicit a pro-angiogenic response *in vitro*

We have previously shown that SEMA4D expression is regulated by the HIF-1 transcriptional complex in HN12 cells and that it promotes endothelial cell chemotaxis *in vitro* and enhanced tumor growth and vascularity *in vivo* [18]. To further study the importance of SEMA4D in the induction of angiogenesis relative to the 'classical' HIF-inducible pro-angiogenic protein VEGF, and to determine if these two factors cooperate in the promotion of angiogenesis, we infected HN cells with control lentiviruses or lentiviruses coding for HIF-1β shRNA. Since HIF-1β is the binding partner for all forms of HIF [27], shRNA-mediated silencing would effectively eliminate HIF-mediated responses in infected cells. We then performed another round of infections with lentiviruses coding for VEGF, SEMA4D, or both, to selectively restore expression of these proteins as shown in the scheme depicted in Fig. 1A, in order to evaluate their individual and combined effects on angiogenesis, tumor growth and tumor vascularity. As expected, HN12 cells infected with lentiviruses expressing HIF-1β shRNA exhibited reduced expression of HIF-1β

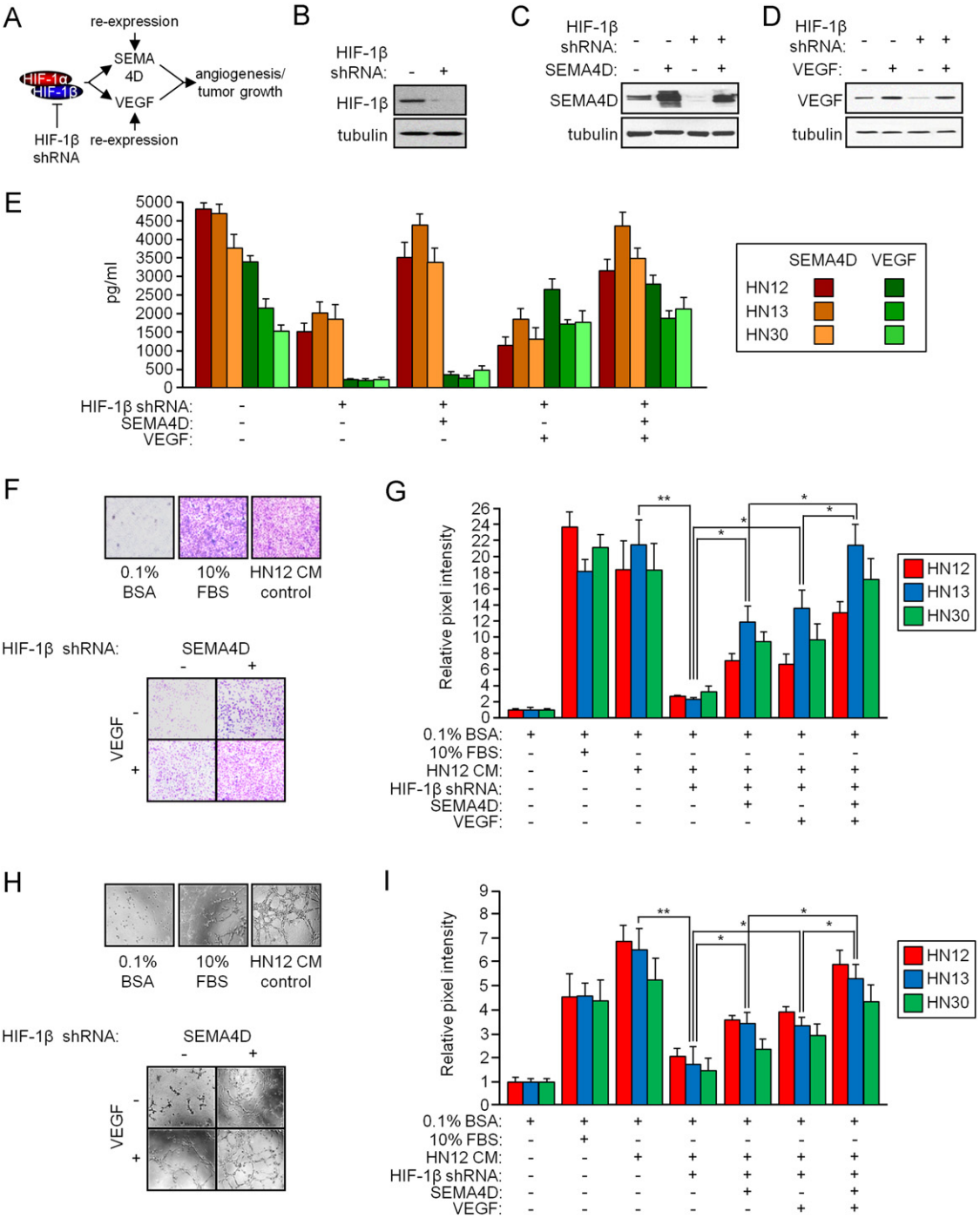

protein (Fig. 1B). These cells also demonstrated reduced levels of the HIF-responsive factors SEMA4D and VEGF as well, but these proteins could be restored in cells co-infected with viruses coding for the appropriate construct (Fig. 1C and D, respectively). We examined by ELISA serum free media conditioned by HN12, 13 and 30 cells infected with lentiviruses expressing HIF-1β shRNA, control co-infected or co-infected with viruses coding for wild-type SEMA4D and VEGF for re-expression of these secreted factors, for eventual use in angiogenesis assays. We detected greatly reduced production of secreted SEMA4D and VEGF released into the media conditioned by cells with silenced HIF-1β relative to controls, but restoration of these factors to levels slightly below that seen in controls (or in the case of VEGF expression in HN30, slightly above) upon co-infection with the appropriate virus (Fig. 1E). Co-infection with viruses expressing both factors restored both to about the levels seen in control infected cells (Fig. 1E). We then used serum free media conditioned by these cells as the chemoattractants for HUVEC in a Boyden chamber migration assay. Media from HN12 infected with HIF-1β shRNA expressing lentiviruses failed to induce a migratory response in HUVEC much higher than that seen in wells containing BSA (negative controls), as these cells likely lost production of most pro-angiogenic factors (Fig. 1F). Restoration of SEMA4D increased HUVEC migration to levels much greater than that of the negative controls, while re-introduction of VEGF exhibited a comparable response (Fig. 1F). Lentiviral-mediated gene transfer of both SEMA4D and VEGF returned cell migration near to the levels seen in control infected cells (Fig. 1F). This assay, performed using HN12, HN13 and 30 cells, is quantified in the bar graph in Fig. 1G. We then performed a tubulogenesis assay, growing HUVEC on reconstituted basement membrane extract (BME) in identical conditions as that used in the migration assay. In media containing FBS (positive control) or conditioned by control infected HN12 cells, HUVEC formed a capillary network, indicative of a pro-angiogenic response, though not when infected with HIF-1β expressing lentivirus (Fig. 1H). Media from HN12 cells where either SEMA4D or VEGF was re-introduced rescued the tubulogenic phenotype slightly, but when combined, VEGF and SEMA4D exhibited a greater response than either pro-angiogenic factor alone (Fig. 1H). Tube formation in media conditioned by identically treated HN12, HN13 and 30 cells is quantified in the bar graph in Fig. 1I. Taken together, these results indicate that HIF-mediated expression of SEMA4D in OSCC can elicit a significant pro-angiogenic response in HUVEC comparable to that induced by VEGF and that together these two factors combine to yield a greater *in vitro* angiogenic phenotype than either factor alone.

Production of SEMA4D by OSCC combines with VEGF to elicit a pro-angiogenic response *in vivo*

To determine if we could detect the effects of HIF-mediated production of SEMA4D by OSCC on angiogenesis *in vivo* and compare the response to VEGF, we performed a directed *in vivo* angiogenesis assay (DIVAA). In this assay, immunocompromised nude mice are implanted with silicon tubes (angioreactors) containing BME mixed with PBS (negative control), VEGF and fibroblast growth factor (VEGF+FGF, positive control), or media conditioned by HN12 cells infected with lentiviruses expressing HIF-1β shRNA and those co-infected with control virus or viruses expressing SEMA4D, VEGF, or both, in order to restore levels of these proteins (Fig. 2A). At the conclusion of the experiment, we observed little blood vessel infiltration into the open end of reactors containing PBS, while those containing VEGF and FGF elicited a strong angiogenic response (Fig. 2A, top row, first and second panels, respectively). Angioreactors containing media conditioned by control infected HN12 cells also elicited a strong angiogenic response, similar to the positive control reactors, which was inhibited in cells where HIF-1β was silenced (Fig. 2A, top row, third and fourth panels, respectively). When expression of SEMA4D or VEGF was restored individually, the mixture of BME with conditioned media from either population rescued a portion of the angiogenic response, while restoration of both factors resulted in recovery of blood vessel growth to a level slightly higher than that seen for the positive control population (Fig. 2A, bottom row). These results are quantified in Fig. 2B, based upon FITC-lectin fluorescence binding to the endothelial cell contents of the reactor [23]. Taken together, these results show that HIF-mediated production of SEMA4D by OSCC cells can elicit a significant pro-angiogenic response *in vivo* similar to that of VEGF and that these factors co-operate to yield a greater angiogenic response than either factor alone.

HIF-mediated production of SEMA4D and VEGF by OSCC cooperates to promote tumor growth, neoplastic cell proliferation and tumor vascularity

Since we observed SEMA4D to be strongly pro-angiogenic both *in vitro* and *in vivo*, promoting endothelial cell migration and blood vessel growth almost as strongly as VEGF, we wanted to assess the relative role of SEMA4D in tumor growth and maintenance of vascularity in xenografts. We used the same populations of cells, control infected, infected with lentiviruses coding for HIF-1β shRNA or expressing HIF-1β shRNA but also SEMA4D, VEGF, or both, as xenografts in immunocompromised nude mice. To ensure that we silenced HIF-1β and suppressed SEMA4D and VEGF expression and could re-express these factors in the xenografts, we examined tissues from the resulting tumors by immunohistochemistry for HIF-1β, VEGF, and SEMA4D. We observed expression of nuclear HIF-1β, along with SEMA4D and VEGF, in control infected cells (Fig. 3A, first column), but reduction or loss of expression of all of these proteins in tumor cells infected *ex vivo* with lentivirus expressing HIF-1β shRNA (second column). Co-infection with viruses coding for SEAM4D, VEGF, or both (Fig. 3B, right three columns, respectively) resulted in re-expression of SEMA4D (middle row) and/or VEGF (bottom row) as detected by immunohistochemistry. A representative sample of tumors harvested at time of sacrifice demonstrates that tumors comprised of HN12 cells with silenced HIF-1β were smaller than controls, once again likely due to an almost complete deactivation of all HIF-mediated survival and growth pathways, while restoration of expression of either SEMA4D or VEGF individually rescued growth (Fig. 3B). Co-expression of both of these factors together resulted in tumor growth exceeding all other populations (Fig. 3B). The volumes of the resulting tumors measured over the course of the experiment also demonstrate this pattern, though statistically significant differences in sizes between tumors with silenced HIF-1β and those

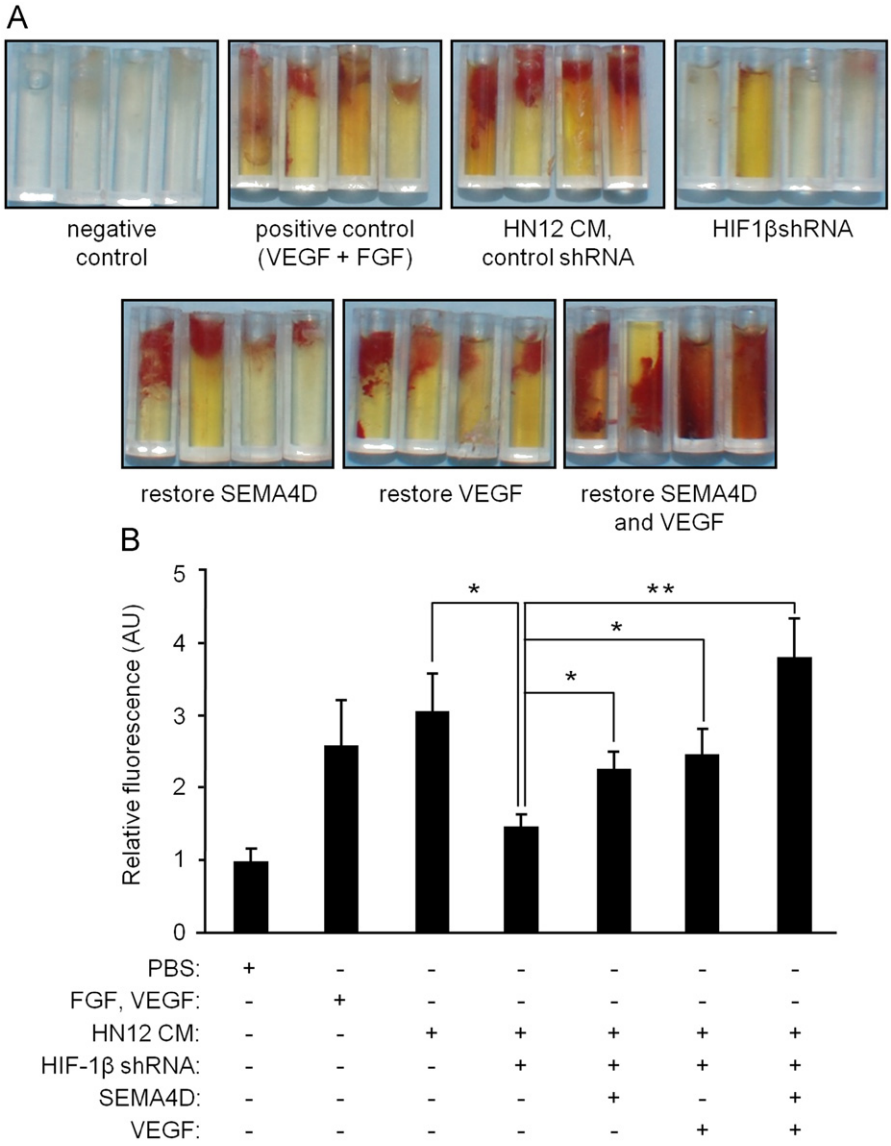

Fig. 2 – HIF-mediated expression of SEMA4D and VEGF by OSCC cooperate to promote a pro-angiogenic response *in vivo*. (A) A DIVAA assay was performed in mice implanted with angioreactors containing reconstituted basement membrane material mixed with PBS (negative control), VEGF and FGF (positive control, VEGF+FGF), or media conditioned by HN12 cells, control infected, infected with lentivirus coding for HIF-1β shRNA, or co-infected with lentiviruses to restore expression of SEMA4D and VEGF. Representative photographs demonstrate blood vessel growth into the open end of the angioreactors. (B) Quantification of blood vessel growth, as measured by FITC-lectin fluorescence (in arbitrary units, AU, *Y*-axis) from endothelial cell contents of each reactor, relative to negative controls. Error bars represent the standard deviation from four reactors (* $p<0.05$; ** $p<0.01$).

with restored SEMA4D and VEGF do not emerge until after day 9 (Fig. 3C). Tumor weights show the size differences more dramatically, as they were taken on the final day of the experiment when size differences were the greatest (Fig. 3D). Knowing the influence of VEGF and SEMA4D on tumor-induced angiogenesis, we processed the tumor tissues for CD31 expression in immunofluorescence to look for vessel content. Silencing HIF-1β reduced vessel content of tumors, as evidenced by reduced CD31 immunofluorescence, compared to tumors comprised of control cells (Fig. 3E). Restoration of SEMA4D or VEGF individually increased blood vessel content, while restoration of both of these factors resulted in tumors containing more vessels than controls (Fig. 3E). These results are shown graphically in Fig. 3F. We then processed the tumors for Ki-67 expression to study the individual effects of these factors on tumor cell proliferation, examining only vital, non-necrotic areas of the histologic sections. Grafts from HIF-1β shRNA infected tumor cells exhibited reduced Ki-67 staining compared to controls (Fig. 3G). Re-expression of SEMA4D increased tumor cell proliferation slightly more than what was seen in tumors re-expressing VEGF, though restoration of both factors resulted in tumor cell proliferation almost identical to that seen in control infected cells (Fig. 3G). These results are shown graphically in Fig. 3H. Taken together, these results indicate that SEMA4D and VEGF are factors regulated by HIF and produced by cells of OSCC for the purposes of supporting tumor cell proliferation through enhanced vascularity.

Anti-SEMA4D therapy combined with VEGF blockade reduces OSCC growth through inhibition of vessel proliferation and maintenance

We have established that OSCC cells express high levels of SEMA4D along with VEGF, under the control of HIF-mediated transcription, and that these factors promote angiogenesis, both *in vitro* and *in vivo*, but combine to significantly enhance tumor growth and vascularity. Therefore, we wanted to determine the value of inhibiting SEMA4D function, concurrent with VEGF blockade, as a way to inhibit tumor vascularity and restrict growth potential. We utilized an anti-SEMA4D blocking antibody

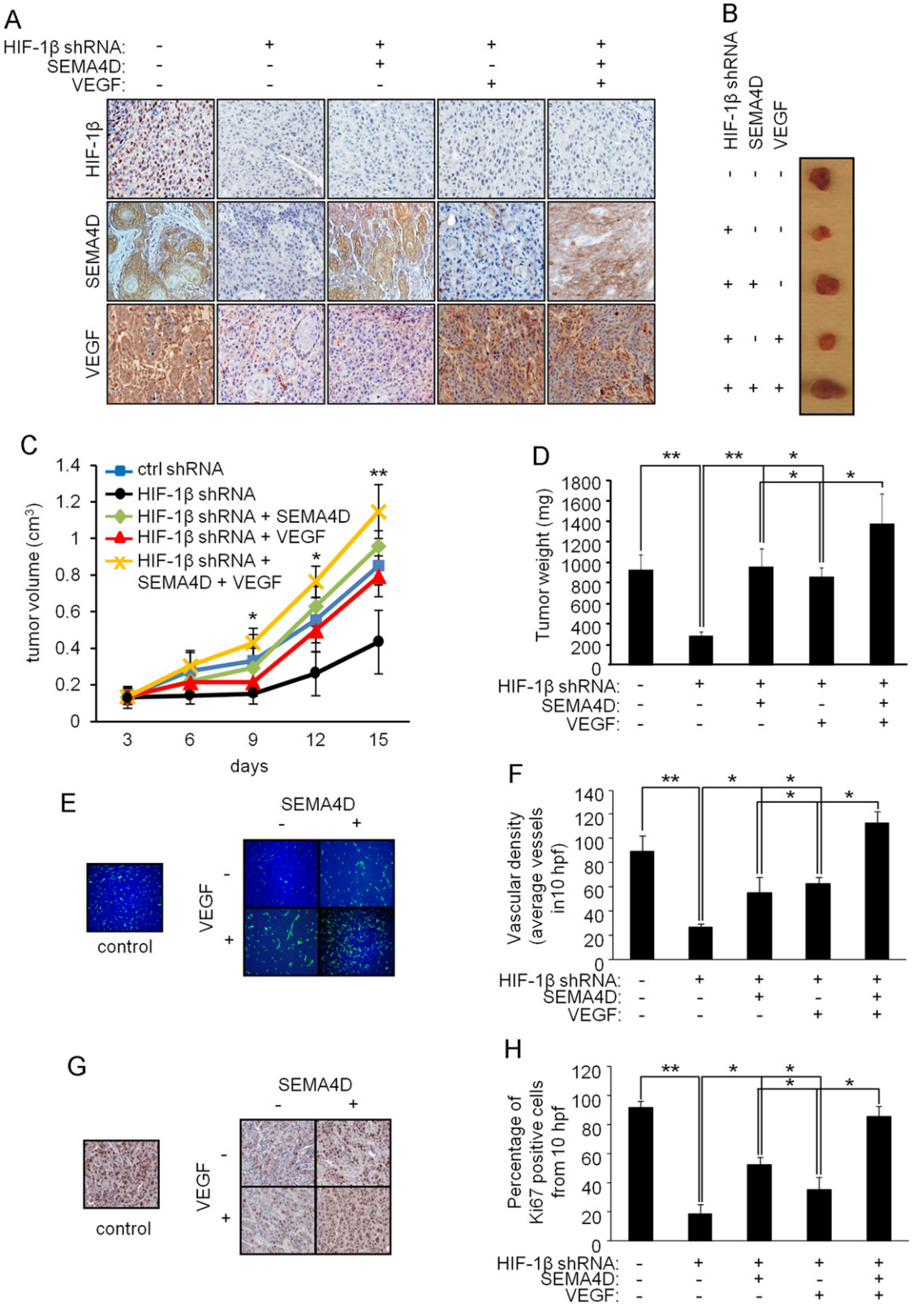

and tested its ability to inhibit SEMA4D binding to its receptor Plexin-B1. We demonstrated that at a concentration of 100 μg/ml, this antibody could specifically block binding of sSEMA4D linked to an alkaline phosphatase (AP) moiety (AP-sSEMA4D) to Plexin-B1 on human umbilical vein endothelial cells (HUVEC) in a binding assay (Fig. 4A). In fact, the blocking antibody was able to reduce the AP response to levels seen in HUVEC infected with lentiviruses coding for Plexin-B1 shRNA, and hence expressing greatly reduced levels of this protein (Fig. S1). Biochemical evidence of inhibition was demonstrated by the ability of the antibody to prevent phosphorylation of ERK, a known downstream effector of Plexin-B1 signaling activated upon ligation by SEMA4D [28] (Fig. 4B). HUVEC also exhibited reduced migration in a Boyden chamber migration assay (Fig. 4C) and tube formation (Fig. 4D) in the presence of sSEMA4D when co-treated with blocking antibody, but not equal concentrations of isotype matched control antibody, demonstrating a specific inhibition of the Plexin-B1-mediated pro-angiogenic response.

We grafted HN12 cells subcutaneously into the flanks of nude mice and administered either IgG isotype matched control antibodies or anti-SEMA4D blocking antibody, anti-VEGF blocking antibody, or both, and measured tumor growth until sacrifice, when tissues were photographed, weighed, and processed for immunohistochemistry and immunofluorescence. As others have observed before, interference with VEGF functioning resulted in a decrease in tumor volume compared to IgG treated controls [29] (Fig. 5A). Administration of anti-SEMA4D blocking antibody resulted in reduced tumor volumes as well, while injections of both antibodies exhibited the greatest restriction in tumor growth (Fig. 5A). Results of volume measurements taken over the entire time course of the experiment demonstrate that tumor growth was suppressed the greatest in mice receiving injections of both blocking antibodies, though statistically significant differences did not appear until day 15, compared to control treated animals (Fig. 5B). Tumor weights taken on the final day of the experiment show these differences more clearly (Fig. 5C). To look at the effects on vascularity, we processed the tumors for CD31 expression in immunofluorescence. Tumors from mice receiving IgG injections were highly vascular, with a similar reduction in vascular content observed in tumors from mice receiving anti-VEGF or anti-SEMA4D antibody treatments (Fig. 5D). Tumors taken from mice treated concurrently with both anti-SEMA4D and anti-VEGF blocking antibodies exhibited the greatest reduction in vasculature (Fig. 5D). These results are quantified in the graph shown in Fig. 5E. We then processed these tumors for Ki-67 to look at tumor cell proliferation. Both antibodies reduced proliferation of tumor cells to similar levels, while combined administration resulted in the greatest reduction of Ki-67 positive nuclei in tumor sections (Fig. 5F, results quantified in the bar graph in Fig. 5G).

VEGF is a unique trophic factor for endothelial cells, promoting endothelial cell proliferation and migration, increasing vascular permeability and inhibiting apoptosis of endothelial cells lining newly formed vessels. To test if SEMA4D also had similar effects on endothelial cell survival, we treated HUVEC with increasing concentrations of sSEMA4D and looked for resistance to apoptosis under conditions of serum starvation. We noted the presence of cleaved, and hence activated, caspase 3 in an immunoblot from serum starved cells, a response which decreased in increasing concentrations of Sema4D, similar to when serum was added to the growth media (Fig. 5H). To test if SEMA4D also had similar effects on endothelial cell survival in tumor tissues, we looked for the presence of active caspase 3 in the vasculature of these tumors in co-immunofluorescence with CD31, as an indicator of endothelial cell apoptosis in vessels. We observed a dense pattern of vascularity (Fig. 5I, CD31, top row, green) and very little cleaved caspase 3 (middle row, red) in IgG control treated tumors (first column) but fewer vessels and much stronger active caspase 3 signal in tumor tissues harvested from mice receiving anti-SEMA4D (second column), which corresponded with CD31 staining in the merged image (bottom row, yellow). Similar results were obtained in tumors from anti-VEGF antibody treated mice (third column). The greatest percentage of active caspase 3 associated with vessels was seen in mice receiving injections of both antibodies (right column, see insets). These results are quantified in the bar graph shown in Fig. 5J. Taken together, the data suggest that SEMA4D and VEGF are produced by OSCC for the purposes of enhancing vascularity, at least partly through protection of endothelial cells against apoptosis, in order to support tumor growth and survival, and that SEMA4D blockade enhances the effects of anti-VEGF therapy.

Fig. 3 – SEMA4D and VEGF production by HN12 cells cooperates to promote tumor growth, neoplastic cell proliferation and vascularity. (A) Immunohistochemistry examining expression of HIF-1β (top row), SEMA4D (middle row) and VEGF (bottom row) in tumor xenografts comprised of control infected cells (first column), cells infected with lentivirus coding for HIF-1β shRNA (second column) and cells infected with lentivirus coding for HIF-1β shRNA but co-infected with virus coding from SEMA4D (third column), VEGF (fourth column) or both (fifth column). (B) HN12 cells, control infected, infected with lentivirus coding for HIF-1β shRNA, or co-infected with lentiviruses to restore expression of SEMA4D and VEGF, as indicated, were injected subcutaneously into nude mice along with a bolus of basement membrane extract. Representative tumors from these xenografts are shown at the time of sacrifice ($n=10$ for each experimental population). (C) The results of tumor volume measurement in cm^3 are shown ($n=10$ for each experimental population; * $p<0.05$; ** $p<0.01$). (D) The results of tumor weights in mg are shown for the last day of the experiment ($n=10$ for each population; * $p<0.05$; ** $p<0.01$). (E) Immunofluorescence for CD31 (green) as a measure of vascular density of tumor populations shown in (A). Nuclei are stained with DAPI (blue). (F) Results of measurement of vascular content from these tumors, determined by the average number of vessels in 10 high-power fields (hpf) of CD31 stained sections (*Y*-axis), quantified in the bar graph (* $p<0.05$; ** $p<0.01$). (G) Immunohistochemistry for Ki-67, to measure proliferation of tumor cells from xenografts shown in (A). (H) Results of Ki-67 staining, expressed as percentage of positive cells observed from 10 high-power fields (hpf). Error bars represent the standard deviation of the averages from three independent experiments (* $p<0.05$; ** $p<0.01$).

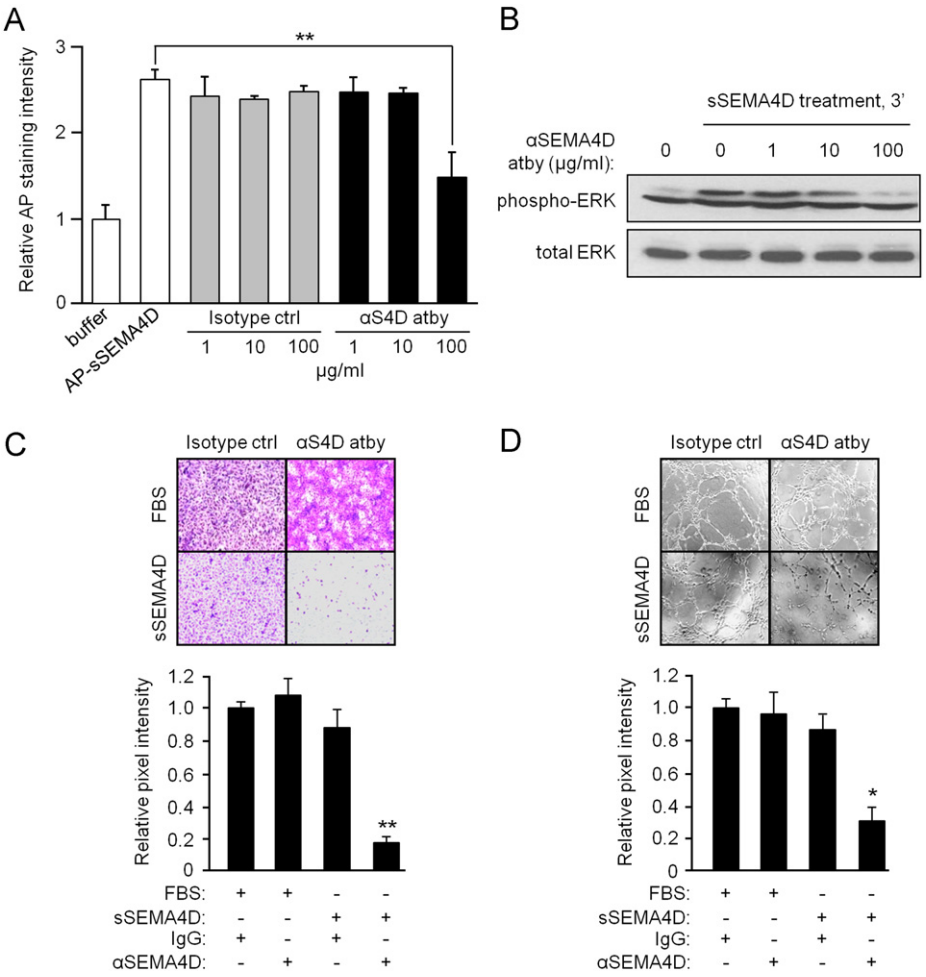

Fig. 4 – Anti-SEMA4D antibody inhibits binding of SEMA4D to Plexin-B1 and activation of Plexin-B1 signaling, and restricts SEMA4D-mediated endothelial cell migration and tubulogenesis. (A) Binding assay of alkaline phosphatase-soluble SEMA4D (AP-sSEMA4D) to HUVEC cells, co-treated with increasing concentrations of isotype control antibody (Isotype ctrl) or anti-SEMA4D blocking antibody (αS4D atby), as measured by AP staining intensity relative to buffer treated cells (*Y*-axis). (B) Phosphorylation of ERK (top panel), a downstream target of activation of Plexin-B1 by SEMA4D binding, is shown in HUVEC incubated with sSEMA4D for 3 min, control treated or treated with increasing concentrations of anti-SEMA4D antibody (αSEMA4D atby). Total ERK is used as the loading control (bottom panel). (C) HUVEC cells were examined in a Boyden chamber for migration toward 10% FBS (FBS, top row), or media containing soluble SEMA4D (sSEMA4D, bottom row), in the presence of isotype control antibody (Isotype ctrl, left column) or anti-SEMA4D blocking antibody (αS4D atby, right column). The results of the migration assay, expressed as pixel intensity of scanned stained migration membranes relative to the FBS and IgG treated cells, is shown in the lower panel. Error bars represent the standard deviation from three independent experiments ($p<0.01$). (D) HUVEC cells were plated on reconstituted basement membrane material in media containing 10% FBS (FBS, top row) or sSEMA4D (sSEMA4D, bottom row), in the presence of isotype control antibody (Isotype ctrl, left column) or anti-SEMA4D blocking antibody (αS4D atby, right column) and examined for formation of capillary tubes. Quantification of the results of the tubulogenesis assay relative to FBS and IgG treated cells, measuring and summing the length of all tubular structures observed in 10 random fields, is shown in the lower panel. Error bars represent the standard deviation from three independent experiments (* $p<0.05$).**

Discussion

HIF-1 drives the transcription or repression of a myriad of genes and pathways important in the coordination of oxygen supply and cellular metabolism. HIF-1 is composed of two polypeptides, HIF-1α and HIF-1β (the aryl hydrocarbon receptor nuclear translocator, or ARNT), with activity of the complex regulated at the posttranscriptional level by hydroxylation and proteasomal degradation of the α subunit [3]. In rapidly growing solid tumors with high metabolic demands or following a series of genetic mutations or other tumorigenic events, together with the influence of inflammatory mediators and other tumor and stromal-released growth factors, degradation of HIF-1α is lost and the HIF-1 transcriptional complex becomes stable and active. In support of this, recent studies have identified increased expression of HIF-1α in many different primary and metastatic tumors, suggesting that its stabilization is a common consequence of a wide variety of mutations underlying human cancer [30].

Active HIF causes a change in tumor cells from an avascular to a neovascular phenotype, an important stage in the evolution of a tumor from an *in situ* disease to one of invasion. Though this adaptation is cell-type-specific and affected by other factors that influence rates of transcription, in general it involves upregulation of pro-angiogenic factors such as VEGF that together comprise a program referred to as the "vascular switch" [31]. So crucial is the vascular switch and production of VEGF for tumor growth, survival, and metastasis that several promising therapeutic interventions have been developed to exploit the dependence of transformed cells on its acquisition. Previously we have shown that SEMA4D is produced by cancer cells under the control of HIF-1 [18], which then strongly promotes tumor growth and vascularity [14], and thus might be a part of this program.

Having demonstrated the role of SEMA4D in tumor-induced angiogenesis, particularly for OSCC, we wanted to systematically evaluate how important this factor was relative to the 'classical' HIF-inducible pro-angiogenic protein VEGF in the context of altered HIF activity, and determine if SEMA4D could represent a new therapeutic target in cancer treatment. Though HIF-1α is the crucial element controlling HIF activity, our approach in these experiments was instead to silence HIF-1β. This novel strategy would result in the inactivation of all HIF isoforms, eliminating the possibility of compensation or cross-talk between family members and inhibiting the entire HIF-induced pro-angiogenic repertoire, which would then allow us to selectively re-express SEMA4D and VEGF through lentiviral mediated gene transfer in order to compare and contrast their effects on promotion of angiogenesis, tumor vasculature, and tumor cell proliferation. Using this approach we demonstrated that the pro-angiogenic properties of tumor-derived SEMA4D rival that of VEGF in HUVEC migration and tube formation *in vitro* and in the promotion of blood vessel growth *in vivo*. In xenografts, SEMA4D production also promoted tumor cell proliferation and vascularity to levels similar to what was observed for VEGF. Importantly, we determined that these two factors together cooperate to promote a greater angiogenic phenotype and more rapid tumor growth than either alone, results that have great clinical implications as we not only could restrict tumor growth and vascularity upon administration of anti-SEMA4D blocking antibody but could cause an even greater inhibition in combination with VEGF blockade. A humanized version of the anti-SEMA4D blocking antibody is currently in development, so our data suggests potential new therapeutic tools for anti-angiogenic treatment of OSCC or other solid neoplasms.

Interestingly, individual restoration of SEMA4D and VEGF yielded somewhat different responses in the assays we performed. We noted a slight but consistent increase in tumor cell proliferation as determined by Ki-67 expression, and slightly greater tumor sizes and weights in xenografts of HIF-1β shRNA expressing cells where SEMA4D was restored compared to VEGF, and a greater loss of tumor cell proliferation when SEMA4D was blocked by antibody. It might be difficult to directly compare the effects of two different ligands, perhaps being secreted by cells at different concentrations, but these results could mean that SEMA4D exerts direct autocrine or paracrine effects on proliferation of tumor cells in addition to its effects on angiogenesis. It has already been suggested that SEMA4D and Plexin-B1 promote tumor cell proliferation through co-activation of the tyrosine kinase receptor Met [32] and there is evidence in the literature that tumors expressing high levels of SEMA4D are more aggressive, more difficult to treat, and have a poor prognosis, not necessarily related to any effect on angiogenesis [33,34]. However, there are also many studies that suggest the opposite. Rody et al. [35,36] have shown that the presence of Plexin-B1 in estrogen receptor positive breast tumors correlates with a favorable prognosis, while other groups have shown that Plexin-B1 acts as a tumor suppressor in melanoma [37], so the issue has not yet been settled.

Though the experiments presented here do not specifically rule out the possibility that SEMA4D or VEGF might act directly on cancer cells, we believe the data argues against autocrine or paracrine signaling contributing significantly to tumor growth. Previously, we have observed a robust *in vitro* angiogenic phenotype and high tumor vascularity in xenografts using HN cell lines that, while expressing high levels of SEMA4D, expressed barely detectable levels of Plexin-B1 [14]. Conversely, we have observed Plexin-B1-dependent migration towards SEMA4D in many cell types that persisted even when the migrating cells failed to express SEMA4D, meaning that cell migration still occurs in a setting where an autocrine or paracrine circuit is disrupted [13,38]. Finally, we have shown that at least for endothelial cells, SEMA4D promotes cell migration but not proliferation [39]. Combined with our current data, these findings suggest that growth of xenografts was not caused by direct effects of tumor SEMA4D acting on Plexin-B1, but instead was due to SEMA4D production by cancer cells promoting chemotaxis of endothelial cells in the microenvironment along a chemical gradient from the existing vascular network of the stroma.

On the other hand, VEGF produced by tumor cells could potentially engage in autocrine signaling with tumor-expressed VEGFR-2, even if SEMA4D and Plexin-B1 do not engage in such a mechanism, a fact that could partly explain some of the differences in cell behavior noted upon restoration of these factors. However, we believe that VEGF also is unlikely to influence HN cells directly. Expression of VEGF receptors in most tumor cells would be a very unusual occurrence, and we have failed to detect VEGFR-2 protein in immunoblots of lysates derived from HN cells in our lab. VEGF could, however, bind to neuropilin (NP)-1, a receptor that is expressed by some tumors [40], but we have not observed any response or change in phenotype for HN cell lines growing *in vitro* in the presence of VEGF (unpublished observations). Instead, VEGF restoration resulted in a small but consistent advantage in promotion of angiogenesis compared to SEMA4D, and a greater decrease in vascularity upon treatment with anti-VEGF antibody, suggesting more endothelial or vascular specific effects on tumor development.

When cells were engineered to over-express both of these factors following HIF inactivation, pro-angiogenic responses and tumor growth and vascularity were greatly stimulated to levels approaching or in some instances exceeding that seen in positive controls or control infected OSCC cells. Such robust responses could be because re-expression of SEMA4D and VEGF resulted in higher protein levels than what was seen for controls, as suggested by the immunoblots in Fig. 1C and D. However, when we examined conditioned media by ELISA for secreted SEMA4D and VEGF in cells engineered to re-express these factors, we observed that protein levels were restored to levels that were actually slightly less than what was seen in control infected cells,

with the exception of VEGF production by HN30 cells, which was slightly higher (though this difference was not statistically significant). Similarly, in an immunohistochemical analysis of tumor xenografts, we observed a decrease in production for both VEGF and SEMA4D upon infection with lentivirus coding for HIF-1β shRNA but re-expression to levels similar to that seen in controls upon co-infection with virus coding for the full length versions of these factors. Taken together, these results suggest that it is more likely that SEMA4D and VEGF together act through parallel pathways initiated by their respective receptors to promote endothelial cell chemotaxis, rather than their effects being related to differences in expression levels.

Once we established the importance of HIF-mediated production of SEMA4D in angiogenesis and tumor growth and survival relative to VEGF, and determined that these factors might be working in tandem to promote such a phenotype, we wanted to establish the value of SEMA4D blockade as part of a possible treatment regimen for OSCC and other solid tumors. Therefore, we employed a blocking antibody reactive to both mouse and human SEMA4D to show that inhibition of SEMA4D binding to

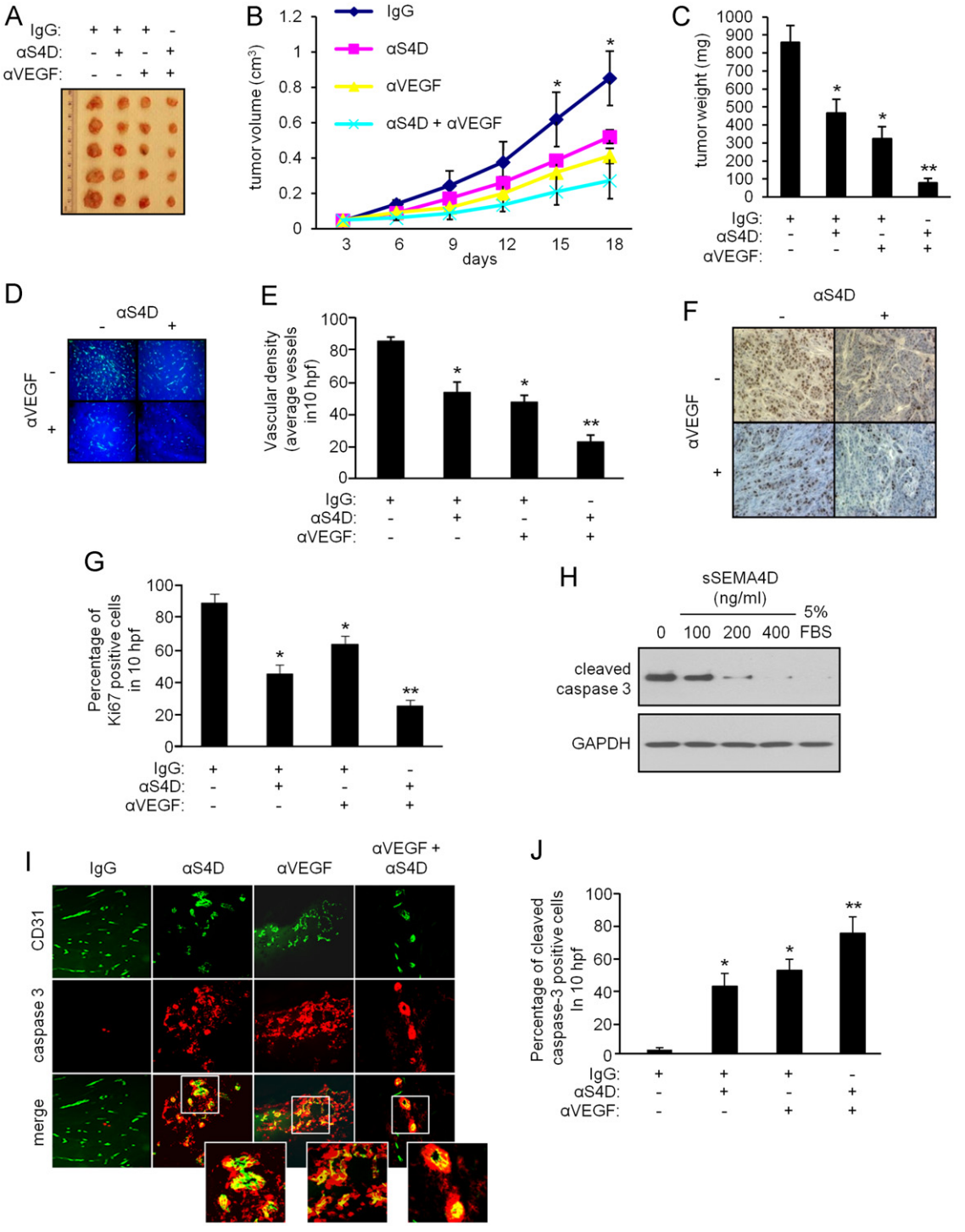

Plexin-B1 resulted in decreased HUVEC migration and tubulogenesis *in vivo* and reduced tumor growth and vascularity *in vitro*. When administered with anti-VEGF blocking antibody, this combined therapy inhibited angiogenesis, growth, malignant cell proliferation and vascularity greater than each antibody alone. We also observed SEMA4D exerting an anti-apoptotic effect over HUVEC growing in low serum and enhanced endothelial cell apoptosis in tumors were both SEMA4D and VEGF were blocked, which when combined with any possible anti-proliferative effects of these therapies resulted in a dramatic restriction in tumor growth. These results suggest that anti-SEMA4D antibody could be combined with VEGF inhibitory approaches in the treatment of OSCC. While combination therapy is known to run the risk of patient toxicity, side effects are unlikely to occur when interfering with the Sema4D/Plexin-B1 system since Plexin-B1 signaling is redundant in normal vascular development and maintenance [41] but as we have shown contributes significantly to angiogenesis in malignancies.

In conclusion we show that SEMA4D and VEGF are produced by HN cells in a HIF-dependent manner, possibly as a result of dysregulated HIF activity, and that these factors combine to elicit a robust pro-angiogenic, pro-survival phenotype in OSCC. Through an individual analysis of its functioning, and by employing novel blocking antibodies, we demonstrate that interference with SEMA4D-mediated pathways could be a viable adjunct to anti-VEGF therapy in the inhibition of pathological angiogenesis.

Acknowledgments

The authors would like to thank Ernest Smith and Maurice Zauderer of Vaccinex, Inc., for providing the anti-SEMA4D antibody and offering technical support, Qiangming Sun of the Institute of Medical Biology, Chinese Academy of Medical Sciences & Peking Union Medical College, for the gift of the VEGF construct, and Daniel Martin and Silvio Gutkind of the National Institute of Dental and Craniofacial Research, NIH, for contributing the head and neck cancer cell lines and assisting in the generation of shRNA lentiviruses. This work was supported by the National Cancer Institute grant R01-CA133162 to J.R.B.

Appendix A. Supporting information

Supplementary data associated with this article can be found in the online version at http://dx.doi.org/10.1016/j.yexcr.2012.04.019.

REFERENCES

[1] L. Mao, W.K. Hong, V.A. Papadimitrakopoulou, Focus on head and neck cancer, Cancer Cell 5 (2004) 311–316.
[2] M.J. Cross, L. Claesson-Welsh, FGF and VEGF function in angiogenesis: signalling pathways, biological responses and therapeutic inhibition, Trends Pharmacol. Sci. 22 (2001) 201–207.
[3] G.L. Wang, G.L. Semenza, Characterization of hypoxia-inducible factor 1 and regulation of DNA binding activity by hypoxia, J. Biol. Chem. 268 (1993) 21513–21518.
[4] K. Tanimoto, Y. Makino, T. Pereira, L. Poellinger, Mechanism of regulation of the hypoxia-inducible factor-1 alpha by the von Hippel-Lindau tumor suppressor protein, EMBO J. 19 (2000) 4298–4309.
[5] M. Uehara, K. Sano, H. Ikeda, M. Nonaka, I. Asahina, Hypoxia-inducible factor 1 alpha in oral squamous cell carcinoma and its relation to prognosis, Oral Oncol. 45 (2009) 241–246.
[6] P.Y. Lin, C.H. Yu, J.T. Wang, H.H. Chen, S.J. Cheng, M.Y. Kuo, C.P. Chiang, Expression of hypoxia-inducible factor-1 alpha is significantly associated with the progression and prognosis of oral squamous cell carcinomas in Taiwan, J. Oral Pathol. Med. 37 (2008) 18–25.
[7] S.Y. Liu, L.C. Chang, L.F. Pan, Y.J. Hung, C.H. Lee, Y.S. Shieh, Clinicopathologic significance of tumor cell-lined vessel and microenvironment in oral squamous cell carcinoma, Oral Oncol. 44 (2008) 277–285.
[8] D.M. Aebersold, P. Burri, K.T. Beer, J. Laissue, V. Djonov, R.H. Greiner, G.L. Semenza, Expression of hypoxia-inducible factor-1alpha: a novel predictive and prognostic parameter in the radiotherapy of oropharyngeal cancer, Cancer Res. 61 (2001) 2911–2916.

Fig. 5 – Anti-SEMA4D therapy combined with VEGF blockade reduces OSCC growth, restricts tumor vascularity, and promotes endothelial cell apoptosis. (A) OSCC tumor xenografts were placed subcutaneously into nude mice treated with IgG control, anti-SEMA4D blocking antibody (αS4D), anti-VEGF blocking antibody (αVEGF), or both. Representative tumors from these xenografts are shown at the time of sacrifice ($n=10$ for each experimental population). (B) The results of tumor volume measurement in cm^3 are shown ($n=10$ for each experimental population; * $p<0.05$). (C) The results of tumor weights in mg are shown ($n=10$ for each experimental population; * $p<0.05$; ** $p<0.01$). (D) Immunofluorescence for CD31 as a measure of vascular density from tumors from mice receiving injections of IgG control antibody, anti-SEMA4D antibody (αS4D), anti-VEGF antibody (αVEGF), or both. Nuclei are stained with DAPI. (E) Results of measurement of vascular content from these tumors, determined by the average number of vessels in 10 high-power fields (hpf) of CD31 stained sections (*Y*-axis), quantified in the bar graph (* $p<0.05$; ** $p<0.01$). (F) Immunohistochemistry for Ki-67, to measure proliferation of tumor cells from xenografts from mice treated with the indicated blocking antibodies. (G) Results of Ki-67 staining, expressed as percentage of positive cells observed from 10 high-power fields (hpf). Error bars represent the standard deviation of the averages from three independent experiments (* $p<0.05$; ** $p<0.01$). (H) Immunoblot performed for the cleaved, active fragment of caspase 3 (top panel) in HUVEC growing under conditions of low serum, treated with the indicated concentrations of sSEMA4D or 5% FBS as a control. GAPDH was used as a loading control (lower panel). (I) Co-immunofluorescence for CD31 (green, top row) and cleaved caspase 3 (red, middle row), to look for co-expression (merge, yellow, bottom row, see also insets) as an indicator of endothelial apoptosis, in tumor xenografts taken from mice treated with IgG control antibody (IgG, first column), anti-SEMA4D antibody (αS4D, second column), anti-VEGF antibody (αVEGF, third column), or both (αS4D+αVEGF, fourth column). (J) Results of vascular apoptosis, expressed as average number of vessels exhibiting cleaved caspase 3 from 10 high-power fields (hpf). Error bars represent the standard deviation of the averages from three independent experiments (* $p<0.05$; ** $p<0.01$).

[9] G. Neufeld, O. Kessler, The semaphorins: versatile regulators of tumour progression and tumour angiogenesis, Nat. Rev. Cancer 8 (2008) 632–645.
[10] A. Kumanogoh, H. Kikutani, The CD100-CD72 interaction: a novel mechanism of immune regulation, Trends Immunol. 22 (2001) 670–676.
[11] K.T. Hall, L. Boumsell, J.L. Schultze, V.A. Boussiotis, D.M. Dorfman, A.A. Cardoso, A. Bensussan, L.M. Nadler, G.J. Freeman, Human CD100, a novel leukocyte semaphorin that promotes B-cell aggregation and differentiation, Proc. Natl. Acad. Sci. USA 93 (1996) 11780–11785.
[12] P. Conrotto, D. Valdembri, S. Corso, G. Serini, L. Tamagnone, P.M. Comoglio, F. Bussolino, S. Giordano, Sema4D induces angiogenesis through Met recruitment by Plexin B1, Blood 105 (2005) 4321–4329.
[13] J.R. Basile, A. Barac, T. Zhu, K.L. Guan, J.S. Gutkind, Class IV semaphorins promote angiogenesis by stimulating Rho-initiated pathways through plexin-B, Cancer Res. 64 (2004) 5212–5224.
[14] J.R. Basile, R.M. Castilho, V.P. Williams, J.S. Gutkind, Semaphorin 4D provides a link between axon guidance processes and tumor-induced angiogenesis, PNAS 103 (2006) 9017–9022.
[15] J.R. Terman, T. Mao, R.J. Pasterkamp, H.H. Yu, A.L. Kolodkin, MICALs, a family of conserved flavoprotein oxidoreductases, function in plexin-mediated axonal repulsion, Cell 109 (2002) 887–900.
[16] C. Siebold, N. Berrow, T.S. Walter, K. Harlos, R.J. Owens, D.I. Stuart, J.R. Terman, A.L. Kolodkin, R.J. Pasterkamp, E.Y. Jones, High-resolution structure of the catalytic region of MICAL (molecule interacting with CasL), a multidomain flavoenzyme-signaling molecule, Proc. Natl. Acad. Sci. USA 102 (2005) 16836–16841.
[17] A. Ventura, P.G. Pelicci, Semaphorins: green light for redox signaling?, Sci. STKE 2002 (2002) PE44.
[18] Q. Sun, H. Zhou, N.O. Binmadi, J.R. Basile, Hypoxia-inducible factor-1-mediated regulation of semaphorin 4D affects tumor growth and vascularity, J. Biol. Chem. 284 (2009) 32066–32074.
[19] M. Cardinali, H. Pietraszkiewicz, J.F. Ensley, K.C. Robbins, Tyrosine phosphorylation as a marker for aberrantly regulated growth-promoting pathways in cell lines derived from head and neck malignancies, Int. J. Cancer 61 (1995) 98–103.
[20] D. Siolas, C. Lerner, J. Burchard, W. Ge, P.S. Linsley, P.J. Paddison, G.J. Hannon, M.A. Cleary, Synthetic shRNAs as potent RNAi triggers, Nat. Biotechnol. 23 (2005) 227–231.
[21] G.J. Hannon, D.S. Conklin, RNA interference by short hairpin RNAs expressed in vertebrate cells, Methods Mol. Biol. 257 (2004) 255–266.
[22] J.R. Basile, K. Holmbeck, T.H. Bugge, J.S. Gutkind, MT1-MMP controls tumor-induced angiogenesis through the release of semaphorin 4D, J. Biol. Chem. 282 (2007) 6899–6905.
[23] L. Guedez, A.M. Rivera, R. Salloum, M.L. Miller, J.J. Diegmueller, P.M. Bungay, W.G. Stetler-Stevenson, Quantitative assessment of angiogenic responses by the directed *in vivo* angiogenesis assay, Am. J. Pathol. 162 (2003) 1431–1439.
[24] G. Sahagun, S.A. Moore, Z. Fabry, R.L. Schelper, M.N. Hart, Purification of murine endothelial cell cultures by flow cytometry using fluorescein-labeled griffonia simplicifolia agglutinin, Am. J. Pathol. 134 (1989) 1227–1232.
[25] L. Laitinen, Griffonia simplicifolia lectins bind specifically to endothelial cells and some epithelial cells in mouse tissues, Histochem. J. 19 (1987) 225–234.
[26] P. Amornphimoltham, V. Sriuranpong, V. Patel, F. Benavides, C.J. Conti, J. Sauk, E.A. Sausville, A.A. Molinolo, J.S. Gutkind, Persistent activation of the Akt pathway in head and neck squamous cell carcinoma: a potential target for UCN-01, Clin. Cancer Res. 10 (2004) 4029–4037.
[27] Q. Ke, M. Costa, Hypoxia-inducible factor-1 (HIF-1), Mol. Pharmacol. 70 (2006) 1469–1480.
[28] J. Aurandt, W. Li, K.L. Guan, Semaphorin 4D activates the MAPK pathway downstream of plexin-B1, Biochem. J. 394 (2006) 459–464.
[29] R. Hasina, M.E. Whipple, L.E. Martin, W.P. Kuo, L. Ohno-Machado, M.W. Lingen, Angiogenic heterogeneity in head and neck squamous cell carcinoma: biological and therapeutic implications, Lab. Invest. 88 (2008) 342–353.
[30] S.J. Welsh, M.Y. Koh, G. Powis, The hypoxic inducible stress response as a target for cancer drug discovery, Semin. Oncol. 33 (2006) 486–497.
[31] G. Bergers, L.E. Benjamin, Tumorigenesis and the angiogenic switch, Nat. Rev. Cancer 3 (2003) 401–410.
[32] S. Giordano, S. Corso, P. Conrotto, S. Artigiani, G. Gilestro, D. Barberis, L. Tamagnone, P.M. Comoglio, The semaphorin 4D receptor controls invasive growth by coupling with Met, Nat. Cell Biol. 4 (2002) 720–724.
[33] E. Ch'ng, Y. Tomita, B. Zhang, J. He, Y. Hoshida, Y. Qiu, E. Morii, I. Nakamichi, K. Hamada, T. Ueda, K. Aozasa, Prognostic significance of CD100 expression in soft tissue sarcoma, Cancer 110 (2007) 164–172.
[34] G. Valente, G. Nicotra, M. Arrondini, R. Castino, L. Capparuccia, M. Prat, S. Kerim, L. Tamagnone, C. Isidoro, Co-expression of plexin-B1 and Met in human breast and ovary tumours enhances the risk of progression, Cell Oncol. 31 (2009) 423–436.
[35] A. Rody, U. Holtrich, R. Gaetje, M. Gehrmann, K. Engels, G. von Minckwitz, S. Loibl, R. Diallo-Danebrock, E. Ruckhaberle, D. Metzler, A. Ahr, C. Solbach, T. Karn, M. Kaufmann, Poor outcome in estrogen receptor-positive breast cancers predicted by loss of plexin B1, Clin. Cancer Res. 13 (2007) 1115–1122.
[36] A. Rody, U. Holtrich, L. Pusztai, C. Liedtke, R. Gaetje, E. Ruckhaeberle, C. Solbach, L. Hanker, A. Ahr, D. Metzler, K. Engels, T. Karn, M. Kaufmann, T-cell metagene predicts a favorable prognosis in estrogen receptor-negative and HER2-positive breast cancers, Breast Cancer Res. 11 (2009) R15.
[37] L. McClelland, Y. Chen, J. Soong, I. Kuo, G. Scott, Plexin B1 inhibits integrin-dependent pp125FAK and Rho activity in melanoma, Pigment Cell Melanoma Res. 24 (2011) 165–174.
[38] N.O. Binmadi, Y.H. Yang, H. Zhou, P. Proia, Y.L. Lin, A.M. Batista De Paula, A.L. Sena Guimaraes, F.O. Poswar, D. Sundararajan, J.R. Basile, Plexin-B1 and Semaphorin 4D Cooperate to Promote Perineural Invasion in a RhoA/ROK-Dependent Manner, Am. J. Pathol. 180 (2012) 1232–1242.
[39] Y.H. Yang, H. Zhou, N.O. Binmadi, P. Proia, J.R. Basile, Plexin-B1 activates NF-kappaB and IL-8 to promote a pro-angiogenic response in endothelial cells, PLoS One 6 (2011) e25826.
[40] A.M. Jubb, L.A. Strickland, S.D. Liu, J. Mak, M. Schmidt, H. Koeppen, Neuropilin-1 expression in cancer and development, J. Pathol. 226 (2012) 50–60.
[41] P. Fazzari, J. Penachioni, S. Gianola, F. Rossi, B.J. Eickholt, F. Maina, L. Alexopoulou, A. Sottile, P.M. Comoglio, R.A. Flavell, L. Tamagnone, Plexin-B1 plays a redundant role during mouse development and in tumour angiogenesis, BMC Dev. Biol. 7 (2007) 55.